J. of Applied Tissue Engineering
2018; 5(4)

Micro-porosity Formation on the Underside of Plasma Sprayed Nickel Splats: A Microstructural Study

Mahmood Meratian[1, 2*], Larry Pershin[1], Javad Mostaghimi[1]

1. Centre for Advanced Coating Technologies, Department of Mechanical and Industrial Engineering, University of Toronto, Toronto, Canada, M5S 1A1
2. Department of Materials Engineering, Isfahan University of Technology, Isfahan 84156-83111, Iran

Received: 02 Jul 2018 / Accepted: 10 November 2018

Abstract:

The gas (micro) porosity formation in splats produced by atmospheric plasma spraying was microscopically studied through a new approach. The aim was to prove hydrogen content in plasma gas mixture propagates micro-porosity to the splat-substrate interface. Nickel powder was sprayed under argon plus 0, 7, 10, and 13 vol.% hydrogen as a secondary plasma gas on a stainless steel substrate, and the obtained microstructures of the underside splats were investigated by a scanning electron microscope. It was shown that by increasing hydrogen concentration in plasma gas mixture, more micro-pores formed in the microstructures, while pores content reached to a saturation level at higher hydrogen concentrations.

Keywords: Atmospheric plasma spray; Micro-porosity formation; Microstructure; Hydrogen gas content; Nickel splats.

Introduction

Atmospheric plasma spraying (APS) is one of the most versatile and rapid techniques to deposit protective metal or nonmetallic coatings onto the surface of components to enhance its properties under severe conditions, improve surface porosity of implants, fabricating low porosity metallic scaffolds and bioceramic coatings on the surface of bioinert metals. The fundamental of the process is heating up the powders above their melting point in a plasma jet and accelerate them toward a substrate. The coating will be formed by the build-up of splats resulting from the impact, flattening, and solidification of melted droplets on the substrate [1]. The coating important properties such as level and distribution of porosity are strongly affected by the in-flight particle conditions [2]. The process has long been considered to be an effective rapid solidification processing, since it allows instant quenching during coating buildup. The microstructures of plasma-sprayed deposits are also ultimately based on the solidification of many individual molten droplets [3]. APS coatings structure usually contain some level of porosity, up to ~10%, some unmelted or partially melted particles, fully melted and deformed "splats," metastable phases, and oxides.

In APS, a plasma gas mixture, which consists of a primary plasma forming gas which is usually argon and a secondary gas, such as hydrogen or helium [1, 4], is introduced into the plasma torch. A high intensity direct current (DC) arc is

generated between the tip of the cathode and the cylindrical anode. A feedstock powder is then injected into high enthalpy, high temperature and velocity jet of partially dissociated and ionized gases emerging from the nozzle. The role of the secondary gas is to enhance the thermal conductivity of plasma for effective heating and melting of the injected powders.

Due to the high temperature and surface area of the particles, any changes in the process parameters can result in significant changes in the particle properties and consequently in the microstructure of the coating [1]. Inspection of the underside of splats often reveals the presence of small gas pores. These pores could be either due to heterogeneous nucleation of absorbed gases in the melt or the result of gas or vapor entrapment under the splat [5]. The size of these pores, however, depends on the mechanism by which they were formed. Entrapment of gas will generate pores which are large (> 1 micron) whereas heterogeneous nucleation generates micro-pores (<< 1 micron). In this paper, we are investigating the latter case, i.e., the heterogeneous nucleation on the underside of the splats.

During its flight towards the substrate, a molten droplet entrains and dissolves plasma gases and the surrounding air. Upon the high velocity impact (>100 m/s) a high transient hydrostatic pressure (approaching 1GPa) established that may rise within ~10^{-8}–10^{-7} s under the droplet [56]. During the depressurization, there will be a point when the absorbed gases will be in supersaturated state and will nucleate. Micro (gas) porosity is generally caused by the evolution of gases during the solidification process. Generally, the solubility of gases in the solid is significantly less than that in the liquid state, and the gases may, therefore, be nucleated during solidification [7]. The solubility of gases in liquids increases nonlinearly with temperature [8]. For nickel and some other metals, a discontinuous and abrupt decrease is observed in the solubility at its melting point of 1453°C (Fig. 1). This will result in a significant generation of micro-pores [8, 9, 10, 11] level of porosity depends on the amount of dissolved gases in the liquid, the type of the metal, chemical kinetics, and the surface tension [7].

The major objective of the present work was to study the effect of hydrogen concentration in the plasma gas mixture on micro-porosity formation on the underside of nickel splats. Commercially pure nickel powder was selected as a model in our experiments since it is main component of many nickel based superalloys used in various high temperature applications. During its flight, the molten nickel particle will absorb some of the hydrogen present in the jet. Upon impact on the substrate, heterogeneous nucleation during solidification is expected to result in generation of micro-pores. This should lead to better understanding and control of micro-porosity formation in the splats, where porosity can be either undesirable or beneficial [12].

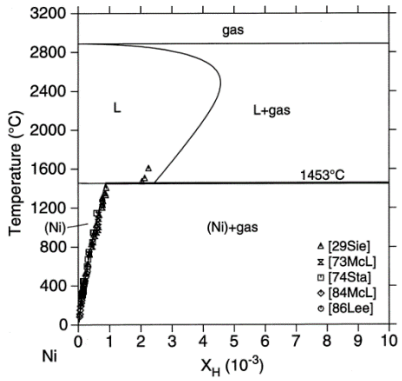

Fig. 1. Ni-rich part of the Ni–H phase diagram, showing hydrogen solubility in liquid and solid states nickel [8]

Material and Methods

Nickel powder (type 12313, Westaim Corp., Edmonton, Alberta, Canada) was used as feedstock material. The initial powder was sieved to make more uniform particle size distribution with the range -45+25 µm. Coatings 200-300 µm thick were deposited on a roughened (0.74µm ±0.04) stainless steel substrates. Roughening was done by 120 grid sand paper manually. In order to suppress splashing of the impacting molten droplets, and time providing for heterogeneous nucleation of micro-pores during the rapid solidification of splats, the substrate temperature was kept at 300 °C by an electric heater. The substrate temperature was measured with a K-type thermocouple.

Nickel powders were deposited by SG-100 DC plasma torch (Praxair/TAFA) sprayed under four different compositions of plasma gases of pure argon and its mixtures with 7, 10, and 13 vol. % of hydrogen. All experiments were done at

120 mm spray distance. During experiments the torch input power was changed in a manner so that particle temperatures remained the same for different H_2 content to provide similar condition for the nickel particles.

Schematic representation of the experimental set up is represented in Fig. 2.

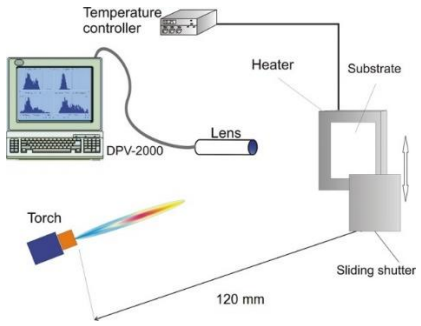

Fig. 2 Schematic of experimental set up

The operating parameters of the torch are listed in Table 1.

Table 1 - Torch Parameters

I [A]	V [V]	Ar [slpm]	H_2 [slpm]	Thermal Efficiency [%]
650	44	60	-	44
420	77	56	4	48
400	77	54	5.6	51
380	79	52	8	52

In-flight particle conditions during experiments, i.e. temperature, diameter, and velocity upon impact shown in Table 2, were measured with a DPV-2000 monitoring system (Tecnar Ltée, Montreal, Quebec, Canada).

Table 2 - Measured in-flight particle conditions during experiments

Sample #	I	II	III	IV
Vol.% of H2 in plasma gas mixture	0	7	10	13
Diameter µm	29 ±4.9	28 ±4.7	27 ±4.6	28 ±4.5
Temperature °C	2360 ±84	2339 ±92	2403 ±89	2326 ±91
Velocity m/s	125 ±12	102 ±16	119 ±17	93 ±15

The splats were removed from the substrates and their underside, i.e., the interface between the splat and the substrate, were studied under scanning electron microscope (SEM) with EDS attachment TM-3000 from Hitachi. The hydrogen content of splats was also measured, by Instrumental Gas Analysis (IGA) (Horiba EMGA-621W). Depending on the Relative Standard Deviation (RSD) obtained, 3 to 5 analytical measurements were done on each sample.

Results

Nickel Particle Feedstock

Fig. 3 shows the morphology of the nickel powder feedstock.

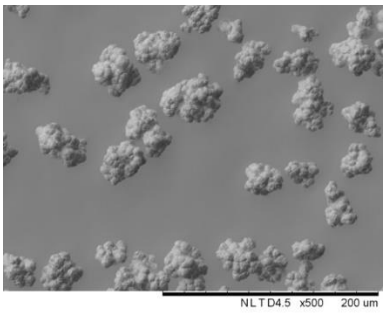

Fig. 3 Nickel powder particles used for plasma spraying

The nodularity of the particles were measured by image analysis and an average aspect ratio of 1.29 ± 0.18 (about 30% deviation from perfect sphere) were obtained. The better nodularity of the nickel particles and size uniformity provide the enhanced flow ability of the powder into the plasma jet, and higher chance for them to be at similar conditions upon impact [13].

Porosity on Splat Microstructures

Fig. 4 shows the microstructure of nickel splat-substrate interface sprayed in pure argon at two different magnifications. Although this case corresponds to pure argon, some micro-porosities are still formed. Our measurements of in-flight particle temperature showed that the particles were superheated above the nickel melting point of 1455°C up to about 2400 °C. The atmosphere around the nickel particle usually contains nitrogen, oxygen, and some moisture. The moisture dissociates at high temperatures and thus can be a source of hydrogen which is easily dissolved in molten droplets with high surface area. Besides, the initial nickel powder was produced by precipitation from a solution

of nickel ammonium sulphate by the introduction of hydrogen gas at high pressure and temperature. Hence, it was possible that some hydrogen dissolve in nickel during production. After particle impact on the substrate, pressure within the drop raises significantly and instantaneously. This is followed by high cooling rate in a range 10^6–10^9 °C/s and a fast drop in pressure. Both of these effects result in nucleation of the dissolved gases. Solidification of the splat then shapes the nucleated gases into micro-pores. It should be noted that the focus of the present study was only on the formation of micro-pores (as shown by arrows in Fig. 4), and the large size pores (> 1 micron) which form due to incomplete filling of the intersplat gaps or due to gas entrapment were not studied.

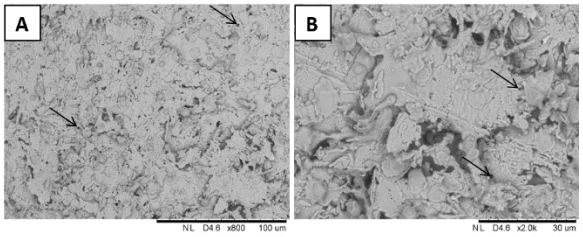

Fig. 4 The microstructure of the splats produced with no H_2 content gas in the plasma atmosphere mixture in different magnifications; A) 800X and B) 2000X

Fig. 5 illustrates the EDS pattern on a single splat underside. Besides the Ni peaks, some oxygen is also observed, this can be attributed to oxidation during flight and cooling on the substrate.

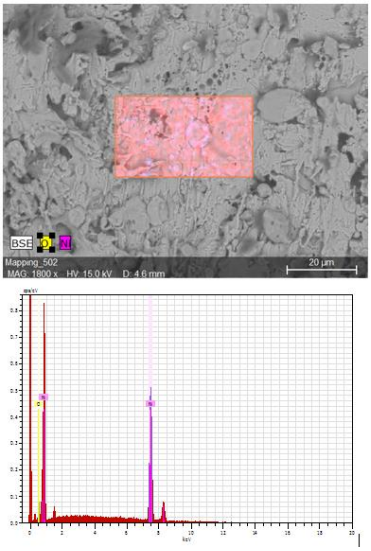

Fig. 5 The EDS spectrum on a single splat produced with no H_2 content gas in the plasma atmosphere mixture showing nickel and oxygen peaks

Fig. 6 illustrates the microstructure of nickel splat interface sprayed in argon with 7% H_2 at different magnifications. Compared to the pure argon case, a higher amount of micro-porosity is scattered throughout the sample (Fig. 6A). In a single splat (Fig. 6B) it was observed that addition of hydrogen to the plasma has considerably increased the number of micro-pores compared to the pure argon case.

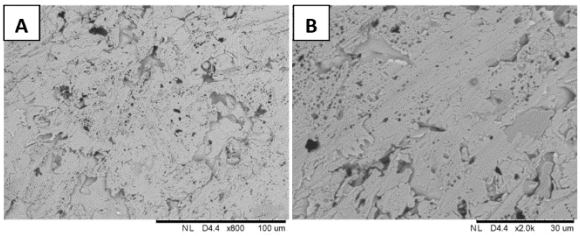

Fig. 6 The microstructure of the splats produced with argon 7% H_2 in the plasma atmosphere mixture in different magnifications; A) 800X and B) 2000X

Fig.7 Shows the EDS pattern for a single splat prepared with argon 7% H_2 in the plasma gas mixture.

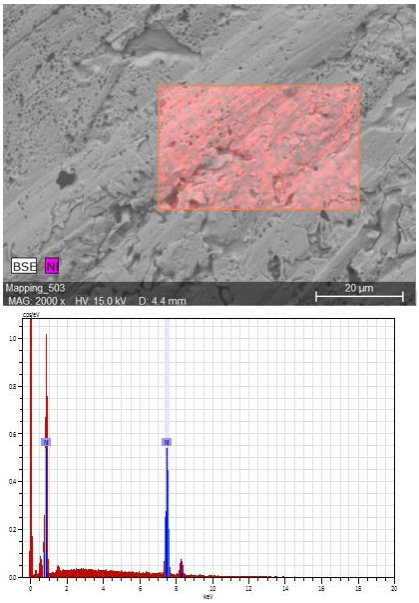

Fig. 7 The EDS spectrum on a single splat produced with 7%H_2 content gas in the plasma atmosphere mixture showing only nickel peaks

In comparison with Fig. 5, no oxygen peak was observed as a result of hydrogen presence, a feature that can be important in some sprayed coatings despite its porosity initiation effect.

Fig. 8 depicts the microstructure of nickel splat-substrate interface sprayed with argon plus 10% hydrogen.

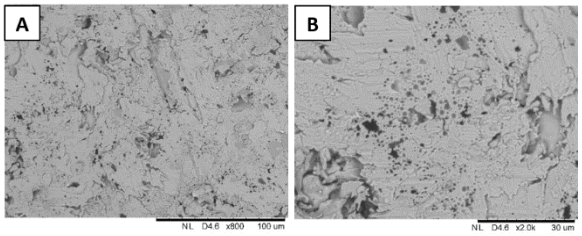

Fig. 8 The microstructure of the splats produced with argon 10% H_2 at different magnifications; A) 800X and B) 2000X

In Fig. 8A larger pores are scattered throughout the sample and, as seen in Fig. 8B, it appears that some pores have merged together. This can cause hydrogen to be more easily released from the samples during cooling period.

Fig. 9 shows the microstructure of nickel splat-substrate interface sprayed with argon plus the extreme case of 13% H_2 in plasma atmosphere at two magnifications. Typically, in plasma spraying processes, 10%H_2 is added to argon as a secondary gas. The selected 13% was to enhance the effect of dissolved hydrogen on the formation of micro-pores.

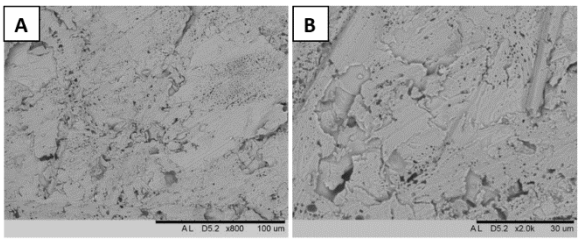

Fig. 9 The microstructure of the splats produced with argon 13% H_2 in the plasma atmosphere mixture in different magnifications; A) 800X and B) 2000X

Comparison Fig. 9 with 13% H2 and Fig. 8 with10% hydrogen shows the same trend in porosity formation. In fact, once the particles converted to molten droplets in plasma jet and during travelling to the substrate target, they exposed to hydrogen gas and due to higher solubility of H2 in molten nickel (Fig. 1), hydrogen was dissolved, and during subsequent cooling and solidification on the substrate micro-pores were nucleated. During cooling and solidification, the rough surface of preheated stainless steel substrate of 300°C provides the nucleation sites, and micro-pores are formed. As the numbers and the density of these pores increase they join together and produce larger pores. This phenomenon also can affect the total H_2 content absorbed by the sample during the process hence higher rate of hydrogen release out of liquid nickel can be expected.

Discussion

In order to support this statement, the samples were analyzed for their hydrogen content and the results presented in Table 3. The table shows maximum, minimum, and average concentration of hydrogen in parts per million (ppm). Also, the results for the RSD% (Relative Standard Deviation), known as the coefficient of variance, is calculated. The RSD is a measure for the precision of average of results. For example, a standard deviation of 6% when average result is 40 would mean that the vast majority of results fall between 34 and 46. The relative standard deviation is widely used in analytical chemistry to express the precision and repeatability of an assay. It is calculated as the following:

[(standard deviation of array X)/ (average of array X)] × 100 = relative standard deviation expressed as a percentage

As it can be seen, the sample produced under no hydrogen content in plasma gas mixture (I) still

Table - 3 Hydrogen analyses of the solid coatings

Sample #	I	II	III	IV
Vol% of H_2 in plasma gas mixture	0	7	10	13
High Rep (ppm)	183	164	198	183
Low Rep (ppm)	101	148	166	170
Avg. (ppm)	134	155	177	178
RSD (%)	22	5.1	10	3.8

contains some hydrogen. As it was mentioned earlier, this could be the reason for lowest level of porosity seen in Fig. 4. Indeed the preheated- roughened stainless steel substrate provided nucleation sites for micro-pores to form in this

sample. Higher RSD% in this sample can be an indication of random hydrogen pick up during powder production.

In subsequent samples, higher amounts of hydrogen contents with lower RSD's can be attributed to hydrogen pick up from plasma gas mixture. Consequently, higher level of porosity is observed on the corresponding microstructures. In the sample IV, the measured hydrogen content ranges to about the same as sample III, in which the microstructures are relatively similar corresponding to their hydrogen content (Fig.'s 8 and 9). It may be that in the latter case, hydrogen bubbles in liquid state merged together and released more H_2 gas as a result of high hydrogen saturation (Fig. 9).

Some other scattering in results obtained could be due to differences in process parameters and droplet properties imposed by plasma spraying route. According to the Table 2, only some minor differences in the impact conditions are observed between the four cases considered here. As it was previously mentioned, after helium, hydrogen has the highest thermal conductivity among gases. Addition of hydrogen will result in faster melting of the injected powder and, hence, more time to dissolve gases before reaching the substrate. In our results this effect reflected in enhancement of torch efficiency by increasing the hydrogen content of the plasma gas mixture despite keeping the particle temperature constant for the sake of similar conditions for the nickel particles throughout the experiments (Table 1).

Conclusion

The influence of hydrogen content in plasma gas mixture on formation of micro-pores on the underside of nickel splats was evaluated microscopically. It was shown microscopically that the higher the amount of hydrogen in the gas mixture, the size and the number of micro-porosities increase while the rate of increasing porosities reaches to a saturation level in higher hydrogen concentrated gas mixtures. All the tests in this work were done on commercially pure nickel, however, due to high differences in hydrogen solubility in liquid and solid states for most commercial metals and alloys, the results can be applicable for them as well.

References

1. Pershin V., Lufitha M., Chandra S. and Mostaghimi J., Effect of Substrate Temperature on Adhesion Strength of Plasma-Sprayed Nickel Coatings. Journal of Thermal Spray Technology. 2003; 12(3): 370-376.
2. Choudhury T. A. , Hosseinzadeh N., Berndt C. C., Artificial Neural Network application for predicting in-flight particle characteristics of an atmospheric plasma spray process. Surface and Coatings Technology. 2011; 205(21–22): 4886–4895.
3. Sampath S., and Herman H., Rapid Solidification and Microstructure Development during Plasma Spray Deposition. Journal of Thermal Spray Technology. 1996; 5(4): 445 – 456.
4. Azarmi F., Vacuum Plasma Spraying. Advanced Materials & Processes. 2005; 163(8): 37- 39.
5. Pfender E., Fundamental Studies Associated with the Plasma Spray Process. Surface and Coatings Technology. 1988; 34: 1-14.
6. Qu M., Wu Y., Srinivasan V. and Gouldstone A., Observations of Nanoporous Foam Arising from Impact and Rapid Solidification of Molten Ni Droplets. Applied Physics Letters. 2007; 90: 254101.
7. Fruehan R. J., Gases in Metals, ASM Handbook, Volume 15: Casting, pp. 64-73, Copyright © 2008 ASM International
8. Kejun Zeng, Klassen T., Oelerich W. and Bormann R., Thermodynamics of the Ni–H System. Journal of Alloys and Compounds. 1999; 283: 151–161.
9. Nakajima H., Ikeda T., and Hyun K. Fabrication of Lotus-Type Porous Metals and their Physical Properties. Advanced Engineering Materials. 2004; 6(6): 377-384.
10. Guang-rui J., Yan-xiang L., Yuan L., Calculation of Hydrogen Solubility in Molten Alloys. Transactions of Nonferrous Metals Society of China. 2011; 21: 1130-1135.
11. MohammadiZahrani M., Meratian M., and Kabiri Y., Innovative Processing of Lotus-Type Porous Magnesium through Thermal Decomposition of Wood. Materials Letters. 2012; 85: 14–17.

12. Introduction to Thermal Spray Processing, Handbook of Thermal Spray Technology, ASM International, 2004

13. Fauchais P., Montavon G., and Bertrand G., From Powders to Thermally Sprayed Coatings. Journal of Thermal Spray Technology. 2010; 19(1-2): 56-80.